Soft Computing (2020) 24:11393–11405
https://doi.org/10.1007/s00500-019-04603-1

METHODOLOGIES AND APPLICATION

An improvement growing neural gas method for online anomaly detection of aerospace payloads

Lei Song[1] · Taisheng Zheng[1,2] · Jianxing Wang[1] · Lili Guo[1,3]

Published online: 12 December 2019

Abstract

The unfluctuating running of on-orbit spacecraft equipment has a decisive impact on the smooth implementation of space exploration mission. However, due to the adverse work conditions and complex running states, it is really a challenge for the online monitoring of aerospace equipment. In this paper, an improved growing neural gas method based on incremental learning is proposed, which is dedicated to solving the problem of online anomaly detection. The learning rate of the proposed method is adaptively adjusted according to the process of model training, ensuring the weights update quickly at the beginning of model construction and converge steady at the end of model training. The optimized insertion mechanisms of neurons ensure that the necessary new neurons are inserted at the right time and location dynamically, while the innovative deletion mechanisms of neurons ensure that the worthless neurons be deleted timely and at the same time guarantee the representation ability of model. The comparison results with the conventional methods on public datasets show that the proposed method achieves the better performance obviously, both in the aspects of detection accuracy and computational efficiency, respectively. At last, as a case study, the proposed method is used for online anomaly detection of a real aerospace device, i.e., a gamma ray detector, and the final F_1 score of anomaly detection is as high as 98.78%. The results show that the proposed method can be applied to online detection of aerospace equipment health conditions effectively.

Keywords Aerospace payloads · Gamma ray detector · Incremental learning · Online monitoring · Anomaly detection

List of symbols

A	Set of all neurons
a	Threshold for the insertion of neurons
a_{m}	Maximum of edge's age
C	The set of edges connecting neurons
c_n	Winning times of the nth neuron
d_p	Distance from the valid set to the model constructed by the parameter set p
e_s	Cumulative error of neuron s
f	F_1 score
N_{d}	Number of samples in data set
N_m	Limitations on the number of nodes
N_w	Threshold for the deletion of isolated neurons
$n(s)$	The set of neurons that connect to the neuron s
p	Precision
p_{s}	Parameter set
$p_{\mathrm{s},0}$	Initial parameter set
r	Recall
s_p	Score of the current parameter
s_x	Anomaly score
t_{d}	Time taken to process all data
v_1	Average velocity of model establishment, dot/s
v_2	Average velocity of anomaly detection, dot/s
w_n	Weight of the winning neuron n
x	The current sample

Communicated by V. Loia.

Lei Song and Taisheng Zheng have contributed equally to this study.

✉ Jianxing Wang
wjx@csu.ac.cn

[1] Key Laboratory of Space Utilization, Technology and Engineering Center for Space Utilization, Chinese Academy of Sciences, Beijing 100094, China

[2] University of Chinese Academy of Sciences, Beijing 100049, China

[3] School of Software, Tsinghua University, Beijing 100084, China

Greek symbols

ε_1	Learning rate of winning neuron
ε_2	Learning rate of neuron in the neighborhood of winning neuron
η_0	Initial learning rate
λ	Step size of inserting neurons
μ	Attenuation coefficient of cumulative error

Abbreviations

CHL	Competitive Hebbian learning
CNN	Convolutional neural network
DNN	Deep neural network
GAN	Generative adversarial networks
GNG	Growing neural gas
ICA	Independent component analysis
LSTM	Long short-term memory
MLP	Multi-layer perception
NG	Neural gas
SAA	South atlantic anomaly
SVM	Support vector machine
FPR	False positive rate
TPR	True positive rate

1 Introduction

With the development of space technology and the aggravation of space exploration tasks, more and more equipment are mounted on spacecraft for space scientific missions. These devices are expensive and difficult to be replaced, and the scientific tasks and data collected by the equipment are of great merit to space science research. Therefore, effective methods are required to monitor the status of equipment. Generally speaking, the working status of equipment is mainly divided into normal and abnormal, so the monitoring of equipment health condition is actually a process of anomaly detection. When the devices are running, an effective anomaly detection algorithm can detect anomalies in advance, and timely measures can be taken to avoid irreparable damages, so as to the unhindered execution of assignments. In recent years, the progress of data mining has provided effective means for equipment abnormal status detection. However, due to the complexity of equipment construction and the unpredictability of operating environment, there are still many challenges in this field: (1) the downlink velocity of equipment status data is high, and it needs to locate outliers quickly under limited computing resources and storage capacity; (2) with the gradual degradation of the devices, the distribution of state data will change, requiring the algorithms to learn the characteristics of new data incrementally; (3) the complex operating environment of equipment requires the algorithms can cope with the complicated relationships of high-dimensional data.

Anomaly detection has been a research hotspot in data mining by virtue of its widespread application in intrusion detection, fault detection, fraud detection, and many other fields. Many algorithms are proposed for anomaly detection according to different requirements. In general, these algorithms can be divided into supervised anomaly detection methods and unsupervised (semi-supervised) ones depending on whether data are labeled or not.

The principal part of supervised anomaly detection algorithms is classification-based methods, which train classifiers with labeled data. Support vector machine (SVM) is a relatively classical method in classification algorithms (Chang and Lin 2011). Wei and Wu (2008) modify the original SVM to build the intrusion detection model, which uses multi-class SVM to classify the features extracted from datasets for detection. And Mukkamala et al. (2002) integrate SVM and multi-layer perception (MLP) to discriminate anomalies and known intrusions. In addition to the adoption of classifiers, Wang and Yang (2019) resolve the problem of feature extraction by supervised independent component analysis (ICA) in order to improve the accuracy of anomaly detection. Recently, deep learning has been effectively applied to anomaly detection of data with complex relationships and achieved remarkable performance. For instance, Lu et al. (2018) propose a novel outlier detection method for the logs of big data systems based on 1D-CNN (convolutional neural network), whose inputs are the features of logs after vector quantization. Ding and Wang (2017) design an intrusion detection model based on deep neural network (DNN), which can effectively distinguish attacks in network data.

Although the supervised anomaly detection methods are effective in most cases, they require a mass of annotated data, which is an intractable problem in practical applications. In addition, the working data of equipment are usually unbalanced, which is not conducive to the training of supervised models. In contrast, unsupervised methods are more impactful in practice.

Traditional unsupervised algorithms can be divided into neighborhood-based methods and clustering-based methods (Chandola et al. 2009). Clustering-based methods are widely used in the field of anomaly detection, whose basic principle is to judge the data that do not belong to any cluster or are away from the existing clusters as abnormal (Li and Niggemann 2017; Celik et al. 2011; Münz et al. 2012). Nevertheless, nearest neighbor-based anomaly detection techniques usually determine whether the current data are abnormal or not according to its neighborhoods.

Angiulli and Pizzuti (2002) obtain anomaly score based on the distance from current instance to its k nearest neighbors. Different from the distance-based methods, Breunig et al. (2000) advocate using density to measure whether the data are abnormal. Besides, one-class SVM is also an optional method (Li et al. 2003). Compared with the traditional unsupervised method, the algorithms based on deep learning are more preferable in feature extraction of complex data. Long short-term memory (LSTM) is extensively applied to the field of outlier detection based on prediction, because of its superiority in processing time series data (Thi et al. 2017; Nguyen et al. 2018), which can estimate whether there are abnormalities in data according to the error between the predicted value and the real one. Different from the prediction-based approaches, Cao et al. (2018) refine the parameters and structure of LSTM to perform anomaly detection of aircraft testing flight data. Generative adversarial networks (GAN) are also an appropriate choice. Schlegl et al. (2019) propose f-AnoGAN, which trains GAN and encoder with normal data and combines the residual error and reconstruction error of images to form anomaly score. And Wang et al. (2018) use similar methods for outlier detection, in which the minimum likelihood regularization is adopted to keep generator from only converging to normal boundary. In addition to the above unsupervised algorithms, autoencoders also have wide range of applications in anomaly detection owing to its excellent performance in feature extraction (Fu et al. 2019; Chen et al. 2018).

Despite the high availability in real-world scenario, the traditional unsupervised approaches cannot perform well in online monitoring of devices in consideration of its dependence on off-line training and the inability in dynamic learning. In contrast, the technique ground on incremental learning is considered to be an alternative for the online renovation of model. Incremental learning is a flexible machine learning strategy, which can learn new patterns from online data and at the same time update the existing model seasonably.

Different algorithms have various trade-offs for preserving historical knowledge, which is the stability-plasticity dilemma problem (Grossberg 1988). Gokcesu et al. (2019) utilize the idea of decision tree to divide the space of observation data into different subspaces and then combines the density function of each subspace to detect anomalies, while as the amount of data increases, decision trees will grow uninterruptedly. Anaissi et al. (2018) propose an adaptive OCSVM for online monitoring of structural health. Yao et al. (2018) combine a new updating strategy of composite nearest neighborhood with LOF to realize online outlier detection. Besides, ART (Postma and Hudson 1995), SOM (Kohonen 1995) and GNG (Fritzke 1994) algorithms all can renew the weights of nodes to adapt to the distribution of new modes. However, both ART and SOM fix the size of model during initialization. The computational complexity of this kind of algorithms is positively correlated with the magnitude of model that can affect the competence of algorithms in the representation of data. It is hard for those algorithms to make a balance between computational complexity and representational capability. Because GNG does not confine the dimension of model in advance, GNG and its variants can incrementally adjust the weights and number of neurons as data changing. However, GNG also has some drawbacks; thus, this paper makes necessary improvements for the purpose of its utility in online anomaly detection of equipment health conditions. The main contributions of this paper are as follows: (1) combine the learning rate with the worthiness of neurons to innovate the adjustment strategy of learning rate in GNG; (2) optimize the mechanisms of neurons addition and deletion, and simplify the structure of model obviously without decrease its performance; (3) the improved algorithm is applied to space equipment condition monitoring, which achieves desirable performance in both detection accuracy and data processing rate.

The rest of this paper is organized as follows. In Sect. 2, the original GNG is introduced briefly, and the optimization strategies of GNG are proposed and described in detail. In Sect. 3, the anomaly detection model based on the improved GNG is constructed. And, in Sect. 4, the effectiveness of the proposed method is verified from the aspects of both detection accuracy and computational efficiency on public datasets, and compared with conventional algorithms. Then, as an engineering case study, anomaly detection is conducted in Sect. 5 on gamma ray dataset based on the proposed method. Finally, we summarize this paper and put forward the focus of the future work in Sect. 6.

2 Improvement of GNG

2.1 Algorithm of original GNG

In this section, the basic theory and process of the original GNG are described briefly, and some improvements of the original GNG are proposed for the algorithm performance.

GNG algorithm consists of neural gas (NG) (Martinetz et al. 1993) and competitive Hebbian learning (CHL), aiming to represent a large amount of data with a limited number of neurons. The idea of NG comes from SOM, which is generally used for data compression and vector quantization. The reason why it is called “Neural Gas” is that in the process of representing data, neurons move like gases in the data distribution space. Hebbian learning was first proposed by Donald Hebb in 1949 as a theory of neuroscience (Hebb 1949). From the view of artificial neural networks, Hebbian learning can be described as a method of determining how to alter the weights between neurons. And competitive learning is a variant of Hebbian learning (Rumelhart and Mcclelland 1986), whose essence is that neurons gain the right to respond to input patterns through competition. The combination of NG and CHL ensures that GNG is capable of both data representation and competitive learning.

The main principles of GNG involve how to adjust weights, how to update the edge-connecting neurons, how to insert and delete neurons. In the process of weights adjustment, GNG uses CHL to update the weights of winning neurons and other neurons in the neighborhood. In terms of edges update, GNG increases the ages of the edges connected to the winning neuron and then deletes the edges beyond the threshold. The removal of edges leads some neurons to become isolated, i.e., there are no edges connect to them. When adding new neurons, GNG measures the importance of neurons by accumulative errors and then adds new neuron between the most important neuron p and the second one q. The weights and cumulative error of the added new neuron are initialized as the corresponding mean values of p and q. In GNG algorithm, the isolated neurons are considered as worthless and will be deleted in priority to simplify the model. The above process makes GNG constantly updating model and adapting to the change of data. The complete GNG algorithm is shown below, and the parameters of algorithm are shown in Table 1:

1. Initialization: $\varepsilon_1, \varepsilon_2, a_{\mathrm{m}}, \lambda, t, A = \{n_1, n_2\}, C = \emptyset, \mu$
2. Input: data stream
3. For each new instance x from the data stream:
4. $t = t + 1$
5. Find the two neurons closest to x from A, which are s and z.
6. Update cumulative error of winning neuron s:

   $$e_s = e_s + \|x - w_s\|^2$$
7. Increase the age of the edges associated with s.
8. Weight adjustment of winning neuron and its neighboring neurons:

   $$w_s = w_s + \varepsilon_1 \times (x - w_s)$$
   $$\forall v \in n(s) : w_v = w_v + \varepsilon_2 \times (x - w_v)$$
9. If s and z are connected by edges, reset the edge's age to 0.
10. Else connect s and z with an edge of age 0:

    $$C = C \cup \{(s, z)\}$$
11. Remove old edges if $a > a_{\mathrm{m}}$.
12. Delete isolated neurons.
13. If $t \ \% \ \lambda = 0$:
14. Let $p = \arg\max_{n \in A} e_n$
15. Let $q = \arg\max_{l \in n(p)} e_l$
16. Create a new neuron r between p and q. The formulas for calculating the related attributes are as follows:

    $$w_r = 0.5 \times (w_p + w_q)$$
    $$e_r = 0.5 \times e_p$$
17. Exponentially decrease the cumulative errors of all neurons:

    $$\forall n \in A : e_n = \mu \times e_n$$

Although GNG can represent massive data with a few neurons, it also has some defects. The main points are as follows: (1) the fixed learning rate in weight adjustment cannot make the model stable gradually; (2) inserting new neurons into the model at every λ steps cannot guarantee that the new neurons are effective to the model; (3) deleting neurons only according to whether the neurons are isolated or not, and some important neurons may be deleted by mistake.

Table 1 Parameters of algorithm

Parameters	The meaning of parameters
A	The set of all neurons
C	The set of edge-connecting neurons
ε_1	The learning rate of winning neuron
ε_2	The learning rate of neuron in the neighborhood of winning neuron
λ	The step size of inserting neurons
$\|x - w_n\|$	The Euclidean distance between x and neuron n
μ	The attenuation coefficient of cumulative error
$n(s)$	The set of neurons that connect to the neuron s
w_s	The weight of neuron s
e_s	The cumulative error of neuron s
a_{m}	The maximum of edge's age

Many algorithms are improved on the basis of GNG, and the improvement strategy mainly includes add–delete mechanism and structure optimization. The main algorithms to improve the mechanism of addition and deletion are GWR, GNG-A, GNG-T and GNG-U. Among them, GWR judges whether new neurons need to be added according to the activity thresholds and firing thresholds of the winning neurons (Marsland et al. 2002); GNG-A uses adaptive forgetting mechanism to identify and delete nodes irrelevant to current data characteristics, and adopts probabilistic evolution mechanism to insert new neurons (Mohamed-Rafik et al. 2018); GNG-T controls the addition and deletion of neurons through T, where T is the sum of current batch errors (FrezzaBuet 2008); GNG-U deletes neurons by adding utility to each neuron (Fritzke 1997). Compared with the above algorithms, SOINN improves the structure and adopts a two-layer network (Furao and Hasegawa 2006). The first layer is similar to the topological representation of GNG, and the second layer further simplifies the topological structure of the first layer by separating low-density overlap. ESOINN is promoted based on SOINN (Furao et al. 2007) and can separate clusters with high-density overlap.

Structural optimization can improve the capability of model, but it also increases computational complexity of algorithms, which make it unsuitable for the application scenarios in this paper, while other variants based on model optimization also have some deficiencies, such as the direct deletion of isolated neurons and the adoption of cumulative error to measure the importance of neurons. Therefore, this paper does not change the layer number of GNG, but improves the method of model updating. The main improvements are as follows: (1) the cumulative error e is removed, and the number of winning c is used to adjust learning rate and control the deletion of neurons; (2) the insertion strategy of neurons is adjusted so that new neurons are added on demand; (3) no longer delete a neuron based on whether it is isolated or not.

2.2 Adjustment strategy of learning rate

The learning rate is an important parameter for training of GNG. In the adjustment process of weights, the learning rate determines the speed at which the weights move to the optimal value. As can be seen from the above algorithm steps, the learning rate is set as constant in the whole training process of GNG, which cannot stabilize the model gradually with the increase in training data.

Given the drawbacks of GNG, the adaptive learning rate is applied in this paper, which can be calculated as follows:

$$\eta_n = \min\left(\eta_0, \frac{1}{c_n + k}\right) \tag{1}$$

where η_0 is the initial learning rate, c_n is the winning times of the nth neuron, k is a constant in the range of [0, 1]. There are two main advantages of using adaptive learning rate, i.e., at the beginning of the model construction, the relatively larger value of learning rate enables the weights to update quickly, while at the end of model training, the gradual attenuation of learning rate enables the neurons with higher winning frequency to converge gradually. In the algorithm of this paper, neurons with more winning times are considered to be more important to the model, and these relatively vital neurons only need small adjustments after lots of incremental learning. So, the dynamic learning rate is conducive to the convergence of existing neurons.

2.3 Insertion strategy of new neurons

Representing a large amount of data with a few nodes is an essential idea of GNG and its variations. However, with the increase in data volume and patterns, it is intractable for the limited number of neurons to ensure the model performance. Therefore, as to this problem, the algorithm should be designed with the ability of inserting new neurons dynamically. But when and where to add new neurons is still a tricky matter. In GNG algorithm, new neurons are inserted between the two neurons with the highest cumulative error at regular intervals, irrespective of whether the time of addition is appropriate, and whether the neurons are redundant. As a result, the model is usually not concise or does not perform well. So, the timing and location of inserting neurons are improved in this paper. When the model does not have enough capacity to represent new patterns, that is, the nearest distance between the current data and the model is larger than the threshold, the algorithm adaptively inserts new neurons to support the new mode. And the insertion location is between the current data and its winning neurons. The weights of new neuron can be calculated as follows:

$$w_i = \frac{w_n + x}{2} \tag{2}$$

where w_i and w_n are the weights of new neuron and the winning neuron n, respectively, and x is the current sample. The purpose of neurons addition is to expand the representation range of the current model. So new neuron is inserted between the new mode and the neurons closest to it, instead of within the scope of current model.

2.4 Deletion strategy of worthless neurons

Neurons deletion can not only simplify the model, but also reduce the complexity of algorithms. But how to guarantee the representation ability of model at the same time is difficult. In GNG algorithm, the neurons that are identified as isolated will be deleted, although the isolated neurons may still be of great significant. GNG-A is more cautious about deleting neurons. Instead of deleting isolated neurons immediately, GNG-A establishes a deletion queue R for isolated neurons. Then the isolated neurons will be retained for a while, and deleted at the appropriate time. Nevertheless, the isolated neurons in queue are only delayed to delete, but will not reactivated again. Identically, the isolated neurons are still considered to be the worthless ones and deleted. In terms of the mechanism of algorithm, the reasons why neurons are isolated may be that the pattern they represent has not appeared for a long time, but the identical pattern may still appear at some time afterward. So, the removals of isolated neurons need to be considered deliberately.

In this paper, the number of winning times instead of the cumulative error is adopted to measure the importance of neurons. The improved algorithm does not delete isolated neurons directly, but removes those with fewer winning times. Moreover, a parameter representing the maximum number of nodes, i.e., N_m is added to prevent the unlimited increase in nodes. When the number of nodes exceeds the threshold, it does not imply that new neurons will not be added any more; instead, those non-isolated neurons with low importance which are not updated for a long time will be considered to remove. The main reasons for choosing the above strategies are as follows: (1) reduce the computational complexity of algorithm while ensuring the presentation ability of model; (2) neurons with high contributions to model should be retained as far as possible.

3 Online anomaly detection model

Anomaly detection refers to quantitatively describing acceptable patterns in order to distinguish patterns that are contrary to normal, so as to achieve the purpose of detection (Chu and Zaniolo 2004). There are various ways to describe acceptable patterns. Clustering-based algorithms use cluster centers to describe acceptable categories, and SVM uses decision boundaries to delineate acceptable regions. After identifying acceptable patterns, there are numerous ways to determine whether the test data are abnormal. For instance, the distance-based methods consider the points which are far away from the normal patterns as abnormal, the density-based methods treat the points which are located in the low-density regions as abnormal, while the probability-based methods regard those points with small occurrence probability as abnormal. Some similar measurement methods can also be used for anomaly detection, such as cosine similarity, grey correlation analysis, and dynamic time warping (DTW) methods, among which the latter two methods can be used for sequences of different lengths.

The improved method in this paper can be divided into two parts: incremental learning and online anomaly detection. In incremental learning part, the algorithm completes the establishment of the model, which mainly includes the update of weights, and the insertion and deletion of neurons. The flowchart is shown in Fig. 1a. By gradually updating, the model follows the topology of data and simplifies its spatial distribution. Further, there is no off-line training during incremental learning. After the completion of incremental learning, the model composed of neurons and edges can represent a large amount of data, which then is used for anomaly detection. In the process of online anomaly detection, the anomaly score is calculated based on the distance between the data and the current model, and the anomaly threshold is used to determine whether the current data are abnormal. The flowchart of anomaly detection is shown in Fig. 1b.

In the process of incremental learning, the improved algorithm in this paper adaptively learns the distribution of data and represents mass data with a simplified topology. In the process of anomaly detection, the distance-based method is used to estimate anomaly state of data, and the anomaly score can be calculated as follows:

$$s_x = e^{-\|x-w_n\|} \tag{3}$$

where x is the current input data, w_n is the weight of the winning neuron n, and $\|x - w_n\|$ is the Euclidean distance of x from its winner. By virtue of Eq. (3), the Euclidean distance of each x and its winner are calculated, and normalized to 0–1 as its anomaly score, using for following anomaly detection.

4 Validation of the proposed method

In the experimental part, four public datasets are introduced, and an artificial dataset is constructed, which are used for validation of the proposed method. The performances of the method proposed in this paper and the conventional algorithms are estimated, and compared in detail.

4.1 Evaluation criteria of algorithm performance

With the purpose of estimating the performance of the proposed method in this paper, some evaluation criteria are introduced in this paper, they are precision p, recall r, F_1 score f, true positive rate (TPR), and false positive rate (FPR), and their formulas are described as follows:

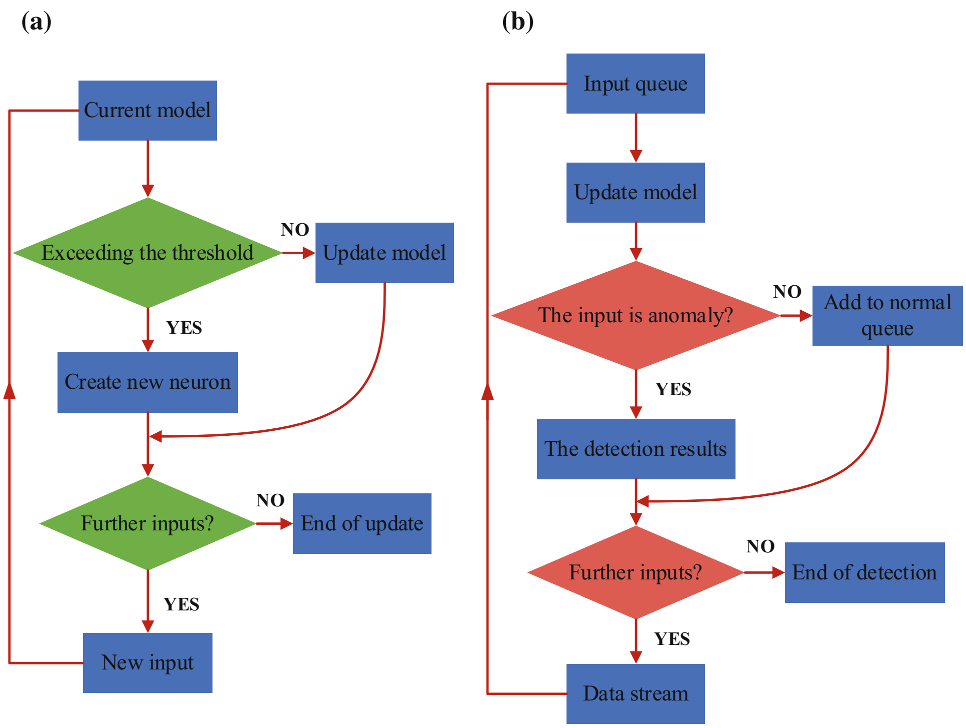

Fig. 1 The process of incremental learning and anomaly detection

$$p = \frac{\mathrm{TP}}{\mathrm{TP} + \mathrm{FP}} \tag{4}$$

$$r = \frac{\mathrm{TP}}{\mathrm{TP} + \mathrm{FN}} \tag{5}$$

$$f = \frac{2 \times p \times r}{p + r} \tag{6}$$

$$\mathrm{TPR} = r \tag{7}$$

$$\mathrm{FPR} = \frac{\mathrm{FP}}{\mathrm{TN} + \mathrm{FP}} \tag{8}$$

$$v = \frac{N_{\mathrm{d}}}{t_{\mathrm{d}}} \tag{9}$$

where TP (true positive) is the number of positive samples that are correctly identified, FP (false positive) is the number of negative samples that are incorrectly identified as positive ones, FN (false negative) is the number of positive samples that are incorrectly identified as negative ones, TN (true negative) is the number of negative samples that are correctly identified, N_{d} is the number of samples in data set, and t_{d} is the time taken to process all data. In this paper, positive samples denote the abnormal samples, while negative samples denote the normal samples.

4.2 Datasets description

Datasets used in this paper are ALOI dataset, shuttle dataset, banknote dataset, kdd99 dataset, and an artificial dataset. Next, the data source, application scenarios, and experimental options of each dataset will be introduced, respectively.

Amsterdam library of object images (ALOI) dataset (Goldstein 2015a): This dataset is a collection of images containing 1000 objects, which is mainly used for target recognition. Each object in ALOI dataset contains 100 pictures that are collected under different perspectives and illumination conditions. The data used in this paper are HSB color histogram features of 50,000 images, among which there are 1500 anomalous samples in all. In the experiment, the number of data in test set is 3000, and the rest are used as the training data.

Shuttle (Statlog Shuttle) Dataset (Goldstein 2015b): This dataset is used to describe the location of the radiators on NASA space shuttle and is mainly used for classification. There are 58,000 samples in the original data set, and 80% of which belong to the first category. The version adopted in this paper has been processed by treating the data belonging to the first category as normal and the rest as anomaly. In the experiment, the test set contains 1700 samples, in which the normal data and abnormal data account for half, respectively.

Banknote Dataset (Dua and Graff 2019): This dataset is extracted from the images in the process of banknote identification, which is used to predict the authenticity of banknotes. Each sample in the dataset contains five attributes. The first four attributes are the features of banknote images obtained by wavelet transform, and the last one is the category. There are 1372 samples in the whole dataset, of which 55.5% are normal samples, and 74% of the normal samples are used as training set

KDD-CUP99 HTTP (Goldstein 2015c): This dataset is a 9-week network connection and system audit data collected from a simulated Air Force LAN, and is often applied to verify the quality of intrusion detection algorithms. To suffice the unsupervised or semi-supervised requirements, a simplified version of KDD99, called KDD-CUP99 HTTP, is finally adopted. KDD-CUP99 HTTP only selects HTTP traffic data in the original dataset, a total of 620,000 samples, of which 1053 are abnormal samples, accounting for 0.17%. In the experiment, 80,000 normal samples were used for training, and 2000 samples for testing.

Artificial dataset: The four public datasets mentioned above are all high-dimensional datasets, while in order to visualize the data distribution patterns, another artificial dataset is constructed in this paper. In the dataset, the data are artificially divided into five categories, and evenly distributed in the two-dimensional space. The algorithms will face the challenges of accurately approximating the data topology, and visualizing the update process of model.

4.3 Visualization of model

The incremental learning algorithms can dynamically update model as data changing, such as SOM, GNG and other algorithms. However, SOM determines the size and structure of the model at the beginning of model establishment, which is different from GNG. The model structure of GNG and its variants does not need to be given artificially. To verify the above statements, and visualize the data topology and update process of model structure, the artificial data are used to train the models, and the structures of each model are recorded at a certain step. Figure 2 shows the artificial data and the topological changes of the three algorithms. As can be seen from Fig. 2, although the structure of three algorithms all changes from simple to complex, the improved method is more concise than the other two methods in terms of data representation. The results also indicate that the optimization of mechanism in improved GNG simplifies the topology of data representation compared with original GNG and GWR.

4.4 Comparison of experiment results

In this paper, a variety of datasets are applied to compare the precision, recall and F_1 scores of each algorithm. In training process, the dataset only contains normal samples, while the test set embraces normal instances and anomalies. Finally, the values of the corresponding evaluation criteria are obtained according to the results on test set and shown in Tables 2, 3, 4 and 5, where the bold fonts denote the best values of each of the criteria of the five methods for each dataset. From the comparison, we come to the conclusion that the improved method achieves good results on the whole. Combining with the results in Fig. 2, it can be found that the improved method can not only simplifies the topology of model, but also does not degrade the performance of anomaly detection.

In addition to high accuracy of anomaly detection, high computational efficiency is also another important requirement for online abnormal detection of devices working conditions. For incremental learning techniques, the time consumed by algorithms is composed of two part, i.e., incremental learning time and abnormal detection time. Due to the disparity of processing time on datasets with different size, the processing rate is adopted in this paper to measure the computational efficiency of each algorithm. However, SOM and K-Means both demand offline training, whose computational efficiency is affected by various factors, including initialization and training batches. Therefore, in the next experiment, the method proposed in this paper is compared with GNG and GWR. The

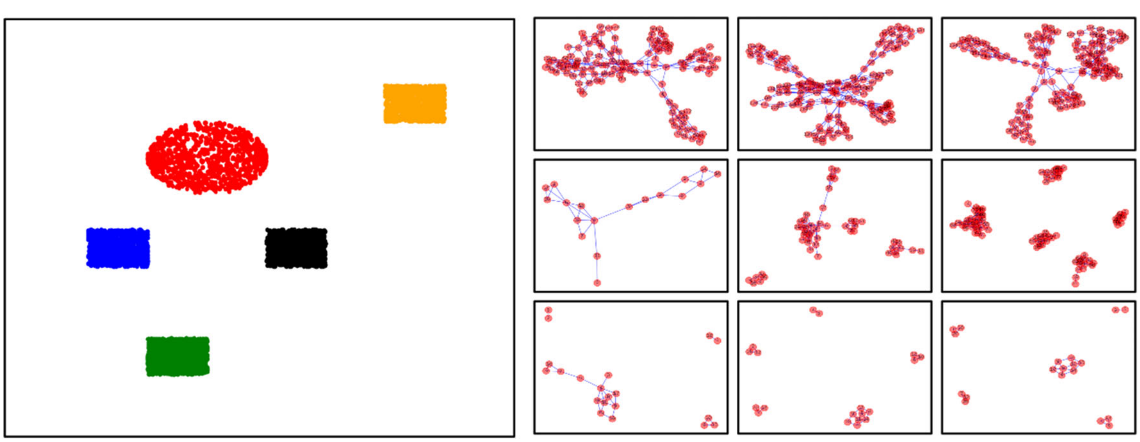

Fig. 2 The topology changes of each algorithm on artificial dataset (from top to bottom are GWR, GNG, and the proposed method)

Table 2 Comparisons of algorithm detection accuracy on ALOI dataset

Criteria	GNG	GWR	SOM	*K*-Means	Proposed method
p	0.5003	0.5056	0.4156	0.5054	**0.5074**
r	0.9907	0.9556	0.2971	0.9549	**0.9993**
f	0.6649	0.6613	0.3465	0.661	**0.6731**

Bold fonts indicate the best values of each criteria of the five methods for ALOI dataset

Table 3 Comparisons of algorithm detection accuracy on Shuttle dataset

Criteria	GNG	GWR	SOM	*K*-Means	Proposed method
p	0.9762	0.9976	0.9976	0.9976	**0.9988**
r	**0.9818**	0.9613	0.9567	0.9612	0.9601
f	0.979	**0.9791**	0.9767	**0.9791**	**0.9791**

Bold fonts indicate the best values of each criteria of the five methods for Shuttle dataset

Table 4 Comparisons of algorithm detection accuracy on Banknote dataset

Criteria	GNG	GWR	SOM	*K*-Means	Proposed method
p	0.9201	0.9800	0.9561	0.9437	**1.0000**
r	0.9443	0.9689	**1.0000**	0.9623	**1.0000**
f	0.9320	0.9744	0.9776	0.9529	**1.0000**

Bold fonts indicate the best values of each criteria of the five methods for Banknote dataset

Table 5 Comparisons of algorithm detection accuracy on KDD-CUP99 HTTP dataset

Criteria	GNG	GWR	SOM	*K*-Means	Proposed method
p	0.9962	0.9981	0.9971	**1.0000**	0.9972
r	0.9981	0.9962	0.9943	0.9943	**0.9990**
f	0.9971	0.9971	0.9957	0.9971	**0.9981**

Bold fonts indicate the best values of each criteria of the five methods for KDD99 HTTP dataset

results are shown in Table 6, where v_1 and v_2 represent the average velocity of model establishment and anomaly detection, respectively, and the bold fonts denote the highest computational efficiency of the three methods on each dataset. The comparison results show that the computational efficiency of the proposed method is superior to that of GNG and GWR in most cases, from both model establishment velocity and anomaly detection velocity.

5 Case study

The effectiveness of the proposed method has been fully verified by comparing with conventional methods, from both detection accuracy and computational efficiency aspects. Then as a case study, the anomaly detection of real engineering dataset is conducted in this section.

5.1 Description of gamma ray detector

The dataset is derived from the sensor of gamma ray detector (gamma ray dataset), which is installed on a real satellite of china for capturing the gamma photons (Toma et al. 2009), and each sample in the gamma ray dataset has 66 parameters, including current, voltage, and temperature, etc. Gamma ray polarimeter mainly consists of two part, that is, polarization detector and electric cabinet. Polarization detector is installed outside the satellite cabin to efficiently capture the gamma photons, while electric cabinet is installed inside of satellite cabin for power supply of detector, control of data transmission, and communication with satellite application system.

The polarization detector consists of two high voltage–power supplying modules, central triggering and concentrator unit, and detecting module, as is shown in Fig. 3a (Xiao et al. 2015). The detecting module consists of 25 detecting units, and the structure of detecting unit is shown in Fig. 3b (Xiao et al. 2015). The gamma photons are firstly captured by plastic scintillator bars, then in the multi-anode photomultiplier the optical signal is transformed into electric signal, with that the electric signal is processed in

Table 6 Algorithm comparison in detection efficiency

Datasets	GNG		GWR		Proposed method	
	v_1 (dot/s)	v_2 (dot/s)	v_1 (dot/s)	v_2 (dot/s)	v_1 (dot/s)	v_2 (dot/s)
ALOI	501.46	658.20	696.76	1042.82	**1001.51**	**2234.64**
Shuttle	453.14	662.89	2744.62	6948.73	**3932.26**	**12,940.62**
Banknote	**1542.30**	5837.08	1100.33	4627.83	1045.32	**6976.25**
KDD99 HTTP	1087.48	2314.91	805.04	943.3	**1535.34**	**2912.21**

Bold fonts denote the highest computational efficiency of the three methods on each dataset

Computer configuration: quad-core Intel core i7 at 2.80 GHz and 8 GB of RAM

Fig. 3 Structure of gamma ray detector. **a** Structure of polarization detector. **b** Structure of one detecting unit

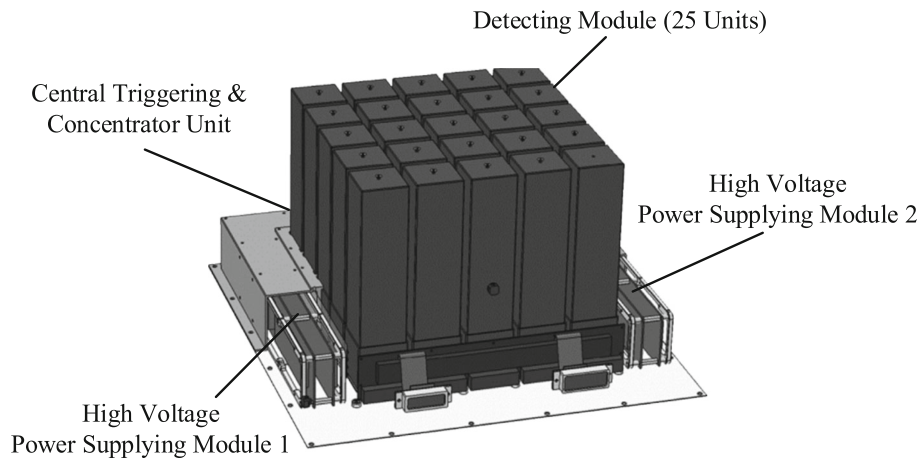

(a) Structure of polarization detector.

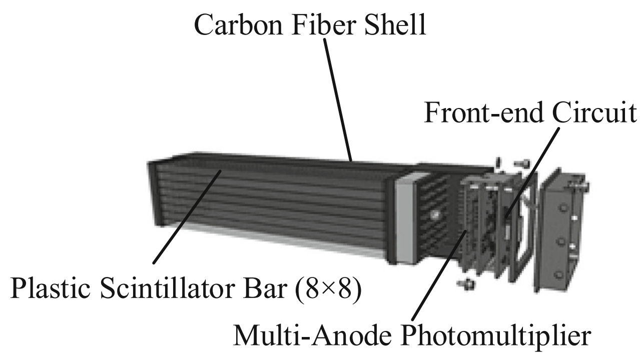

(b) Structure of detecting unit.

the front-end circuit, and the effective part is finally chosen.

As described above, gamma ray detector consists of many precise parts; besides, it has been suffering from adverse work conditions, such as space microgravity, single-event upsets, and so on. Actually, there was once a malfunction on the gamma ray detector in its service period. Although all components were run under the requirement of design, and the corresponding parameters had not exceeded the design thresholds, the gamma ray detector still suffered from identified malfunction and failed to startup at last. After the event, according to comprehensive analysis of a large number of experts, some parameters of the monitoring parameters were considered to be abnormal before the failure, for instance, high voltage–power state, auxiliary power state, electric current, and so on.

Take the most obvious abnormal parameter, electric current, as example. As is shown in Fig. 4, the threshold value of electric current, according its design requirement, is [0, 2] A. And in the course of daily operation, the current of detector is about 1.44 A, while when it enters the South Atlantic Anomaly (SAA) area, the current of detector is about 1.24 A. As can be seen from Fig. 4, at the last time the detector left the SAA area, the current of detector was increased to about 1.52 A, and 80 min later, the detector never worked again. Unfortunately, this serious failure was failed to be detected by the existing monitoring and alerting system. The most important reason is that, all of the 66 parameters, even the electric current, still had not exceeded the design thresholds, so the alerting system was not activated. And the second, although by expert analysis the electric current was finally considered to be abnormal, it cannot be identified accurately and timely by human when the anomaly occurred. So, an accurate and effective method is very necessary for online anomaly detection of gamma ray detector.

As a very valuable case, the operation data before malfunction will be studied by the proposed method in this section, for the purpose of accurate anomaly detection and fault alert during its following service, and ensure safe

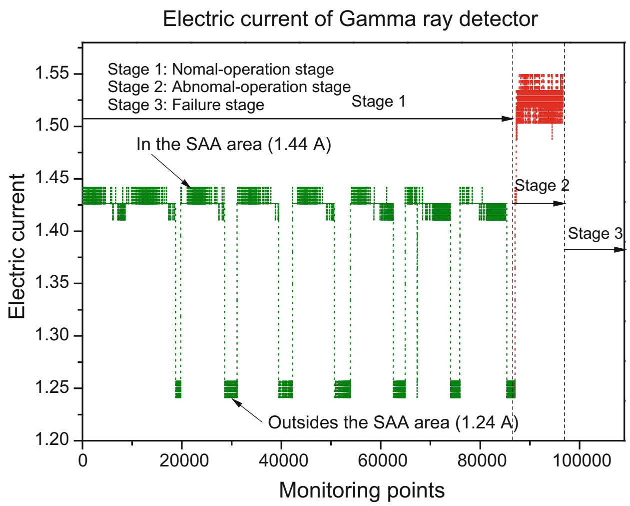

Fig. 4 Division of the gamma ray detector work stage

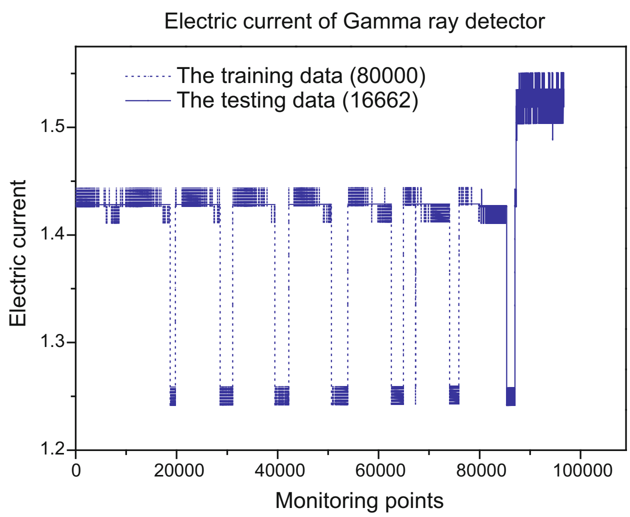

Fig. 5 Division of the training data and testing data

operation of the gamma ray detector by necessary measures. According to the analysis result of experts, the operation conditions of gamma ray detector are divided into three stages, i.e., normal-operation stage, abnormal-operation stage, and fault stage, as shown in Fig. 4. In this paper, the data before the fault stage are used for anomaly detection by the proposed method; the goal is to detect anomalies timely and accurately in the second stage, i.e., the abnormal-operation stage.

A total of 96,662 samples are collected in the data set; in the experiment, 80,000 normal samples were selected as the training set, and the rest are used for test. The division of training data and testing data is shown as Fig. 5.

Table 7 Parameters of the proposed method

Parameters	The meanings of parameters
a	The threshold for the insertion of neurons
a_{m}	The maximum of edge's age
N_m	Limitations on the number of nodes
N_w	The threshold for the deletion of isolated neurons

5.2 Initialization of model

Quality of initialization parameters has a great impact on the performance of the model. Therefore, the initialization parameters should be set reasonably. In this paper, the average distance from the validation set to model is used to evaluate the performance of each set of initialization parameters, and the corresponding score can be calculated as follows:

$$s_p = e^{-d_p} \tag{10}$$

$$d_p = \frac{1}{N_{\mathrm{v}}} \sum_{x \in V} \|x - w_n\| \tag{11}$$

where d_p is the average distance from the validation set to the model constructed by the parameter set p, s_p is the score of the current parameter set, V and N_{v} correspondingly represent the validation set and the number of samples in validation set, x is a sample from V, w_n is the weight of the winning neuron n, and $\|x - w_n\|$ is the Euclidean distance of x from w_n.

According to Eq. (10), the score of parameters is negatively correlated with average distance, i.e., the smaller the average distance, the higher the score of parameters. The parameters, i.e., a, a_{m}, N_m, and N_w, in the proposed method are explained in Table 7, respectively. Among these parameters that need to be initialized cautiously, N_m

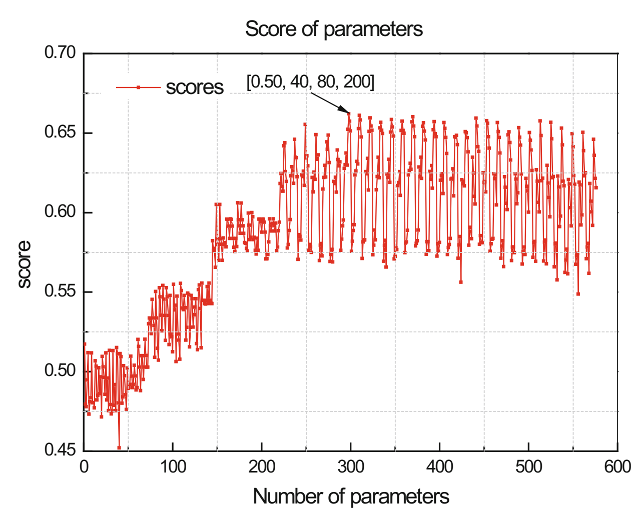

Fig. 6 The score of parameters in algorithms

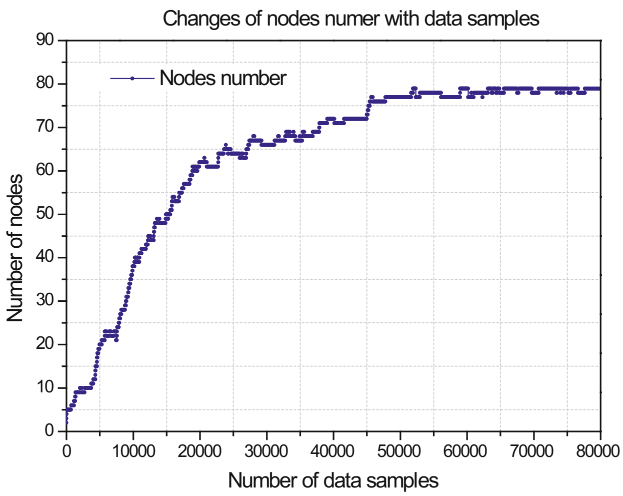

Fig. 7 Changes in the number of model's neurons

Table 8 Performance of the proposed method on gamma ray dataset

Criteria	p	r	f	v_1 (dot/s)	v_2 (dot/s)
Value	0.9771	0.9987	0.9878	828.78	1829.47

limits the number of neurons in the model, and N_w controls the removal of isolated neurons. If the winning times of isolated neurons that have not been updated for a long time are less than N_w, then the isolated neuron will be eliminated. All combinations of parameters are traversed with a certain step size in their ranges, and the scores of corresponding parameters are obtained according to Eq. (10) and shown in Fig. 6. It can be seen that, when the initial parameters set for the proposed method is $p_{s,0} = [0.5, 40, 80, 200]$, the corresponding score reaches its maximum; then p_0 is chosen as the initialization parameters.

5.3 Results and analyses

The number of neurons in the proposed model is recorded with the increase in data, as is shown in Fig. 7; the number of neurons is eventually stabilized at about 80, i.e., the size of the model tends to be steady quickly, instead of growing immoderately, which is significant for the control of model complexity.

At last, the final results are shown in Table 8. It can be seen that, as to the detection accuracy, the precision is 97.71%, the recall is 99.87%, and the F_1 is as high as 98.78%. And, as to the detection speed, the v_1 and v_2 are 828.78 dot/s and 1829.47 dot/s, respectively. The final results show that both detection accuracy and efficiency of the proposed method are all meet the requirement of online anomaly detection of gamma ray detector.

6 Conclusions

An improvement GNG method is proposed for online anomaly detection of gamma ray detector in this paper. The learning rate updates adaptively, and the addition and deletion mechanisms of neurons are both optimized. Then the improved GNG method is verified on public datasets and artificial dataset by comparing with conventional methods, from both detection accuracy and computational efficiency aspects. For practical application, the improved GNG method is finally used for anomaly detection of a real aerospace gamma ray detector. The main conclusions can be summarized as follows:

1. An improvement GNG method is proposed in this paper for online anomaly detection of aerospace payloads.
2. The update strategy of learning rate, and addition and deletion mechanisms of neurons are optimized reasonably.
3. Both detection accuracy and computational efficiency of the proposed method are improved obviously compared with conventional methods.
4. The proposed method can be effectively used for online anomaly detection of gamma ray detector, and the final F_1 score of anomaly detection is as high as 98.78%.

For future work, integrating multiple incremental learning algorithms to address online anomaly detection of space payloads is a worthy topic. Moreover, how to judge whether new data are beneficial to the existing model based on detected results is also important that need to be considered.

Acknowledgements The dataset of gamma ray detector in this work is provided by Chinese Manned Space Flight Project. This study has been supported by the Foundation of Key Laboratory of Space Utilization, Technology and Engineering Center for Space utilization, Chinese Academy of Sciences (No. CSU-QZKT-2018-09) and the Open Project of Beijing key Laboratory of Measurement and Control of Mechanical and Electrical System (No. KF20181123205), China.

Compliance with ethical standards

Conflict of interest The authors declare that they have no conflict of interest.

Ethical approval This article does not contain any studies with human participants or animals performed by any of the authors.

References

Anaissi A, Khoa NLD, Rakotoarivelo T et al (2018) Adaptive online one-class support vector machines with applications in structural health monitoring. ACM Trans Intell Syst Technol 9(6):1–20

Angiulli F, Pizzuti C (2002) Fast outlier detection in high dimensional spaces. In: Principles of data mining and knowledge discovery, 6th European conference, PKDD 2002, Helsinki, Finland, 19–23 Aug 2002. Proceedings. Springer

Breunig MM, Kriegel HP, Ng RT et al (2000) LOF: identifying density-based local outliers. ACM Sigmod Rec 29(2):93–104

Cao Z, Zhu Y, Sun Z et al (2018) Improving prediction accuracy in LSTM network model for aircraft testing flight data. In: 2018 IEEE international conference on smart cloud (SmartCloud). IEEE, pp 7–12

Celik M, Dadasercelik F, Dokuz AS (2011) Anomaly detection in temperature data using DBSCAN algorithm. In: International symposium on innovations in intelligent systems and applications. IEEE

Chandola V, Banerjee A, Kumar V (2009) Anomaly detection: a survey. ACM Comput Surv 41(3):15

Chang CC, Lin CJ (2011) LIBSVM: a library for support vector machines. ACM Trans Intell Syst Technol 2:1–27

Chen Z, Yeo CK, Lee BS et al (2018) Evolutionary multi-objective optimization based ensemble autoencoders for image outlier detection. Neurocomputing 309:192–200

Chu F, Zaniolo C (2004) Fast and light boosting for adaptive mining of data streams. Lect Notes Comput Sci 3056:282–292

Ding S, Wang G (2017) Research on intrusion detection technology based on deep learning. In: 2017 3rd IEEE international conference on computer and communications (ICCC). IEEE, pp 1474–1478

Dua D, Graff C (2019) UCI machine learning repository. University of California, School of Information and Computer Science, Irvine

FrezzaBuet H (2008) Following non-stationary distributions by controlling the vector quantization accuracy of a growing neural gas network. Elsevier, Amsterdam

Fritzke B (1994) A growing neural gas network learns topologies. In: International conference on neural information processing systems. MIT Press

Fritzke B (1997) A self-organizing network that can follow non-stationary distributions. In: International conference on artificial neural networks. Springer, Berlin, pp 613–618

Fu X, Luo H, Zhong S et al (2019) Aircraft engine fault detection based on grouped convolutional denoising autoencoders. Chin J Aeronaut 32(2):296–307

Furao S, Hasegawa O (2006) An incremental network for on-line unsupervised classification and topology learning. Neural Netw 19(1):90–106

Furao S, Ogura T, Hasegawa O (2007) An enhanced self-organizing incremental neural network for online unsupervised learning. Neural Netw 20(8):893–903

Gokcesu K, Neyshabouri MM, Gokcesu H et al (2019) Sequential outlier detection based on incremental decision trees. IEEE Trans Signal Process 67(4):993–1005

Goldstein M (2015a) Unsupervised anomaly detection benchmark, V1 edn. Harvard Dataverse (aloi-unsupervised-ad.tab)

Goldstein M (2015b) Unsupervised anomaly detection benchmark, V1 edn. Harvard Dataverse (shuttle-unsupervised-ad.tab)

Goldstein M (2015c) Unsupervised anomaly detection benchmark, V1 edn. Harvard Dataverse (kdd99-unsupervised-ad.tab)

Grossberg S (1988) The ART of adaptive pattern recognition by a self-organizing neural network. Computer 21:77–88

Hebb DO (1949) The organization of behavior, vol 65. Wiley, New York

Kohonen T (1995) Self organizing maps. Ser Inf Sci 30(4):266–270

Li P, Niggemann O (2017) Improving clustering based anomaly detection with concave hull: an application in fault diagnosis of wind turbines. In: IEEE international conference on industrial informatics. IEEE

Li KL, Huang HK, Tian SF et al (2003) Improving one-class SVM for anomaly detection. In: International conference on machine learning and cybernetics. IEEE

Lu S, Wei X, Li Y, Wang L (2018) Detecting anomaly in big data system logs using convolutional neural network. In: 2018 IEEE 16th international conference on dependable, autonomic and secure computing, 16th international conference on pervasive intelligence and computing, 4th international conference on big data intelligence and computing and cyber science and technology congress (DASC/PiCom/DataCom/CyberSciTech), Athens, pp 151–158

Marsland S, Shapiro J, Nehmzow U (2002) A self-organising network that grows when required. Neural Netw 15(8):1041–1058

Martinetz TM, Berkovich SG, Schulten KJ (1993) Neural-gas' network for vector quantization and its application to time-series prediction. IEEE Trans Neural Netw 4(4):558–569

Mohamed-Rafik B, Slawomir N, Payberah AH (2018) An adaptive algorithm for anomaly and novelty detection in evolving data streams. Data Min Knowl Discov 32(6):1597–1633

Mukkamala S, Janoski G, Sung A (2002) Intrusion detection using neural networks and support vector machines. In: International joint conference on neural networks. IEEE

Münz G, Li S, Carle G (2012) Traffic anomaly detection using *K*-means clustering. In: GI/ITG Workshop MMBnet, pp 13–14

Nguyen VQ, Van Ma L, Kim J et al (2018) Applications of anomaly detection using deep learning on time series data. In: 2018 IEEE 16th international conference on dependable, autonomic and secure computing, 16th international conference on pervasive intelligence and computing, 4th international conference on big data intelligence and computing and cyber science and technology congress (DASC/PiCom/DataCom/CyberSciTech). IEEE, pp 393–396

Postma EO, Hudson PTW (1995) Adaptive resonance theory. In: Artificial neural networks. Springer, Berlin, Heidelberg, pp 101–117

Rumelhart DE, Mcclelland JL (1986) Parallel distributed processing, vol 1. MIT Press

Schlegl T, Seebock P, Waldstein SM, Langs G, Schmidt-Erfurth U (2019) f-AnoGAN: fast unsupervised anomaly detection with generative adversarial networks. Med Image Anal 54:30–44

Thi NN, Cao VL, Le-Khac N-A (2017) One-class collective anomaly detection based on LSTM-RNNs. In: Transactions on large-scale data-and knowledge-centered systems XXXVI. Springer, Berlin, Heidelberg, pp 73–85

Toma K, Sakamoto T, Zhang B et al (2009) Statistical properties of Gamma-ray burst polarization. American Institute of Physics, American Astronomical Society, Washington

Wang GP, Yang JX (2019) SKICA: a feature extraction algorithm based on supervised ICA with kernel for anomaly detection. J Intell Fuzzy Syst 36(1):761–773

Wang C, Zhang YM, Liu CL (2018) Anomaly detection via minimum likelihood generative adversarial networks. In: 2018 24th International conference on pattern recognition (ICPR). IEEE, pp 1121–1126

Wei YX, Wu M-Q (2008) KFDA and clustering based multiclass SVM for intrusion detection. J China Univ Posts Telecommun 15(1):123–128

Xiao H, Dong Y, Wu B, Zhang S et al (2015) Gamma ray polarimeter POLAR of TG-2. Manned Spaceflight 2015:21

Yao H, Fu X, Yang Y et al (2018) An incremental local outlier detection method in the data stream. Appl Sci 8(8):1248